https://doi.org/10.1590/jatm.v18.1465 ORIGINAL PAPER

Multidisciplinary Optimization of Power Device Sizing to Improve Flight Duration and Weight Reduction of Solar-Powered Aircraft

Bashir Danjuma Safyanu[1,*], Zamri Bin Omar[2], Mohd Noor Abdullah[3]

1. Universiti Tun Hussein Onn Malaysia – Faculty of Mechanical and Manufacturing Engineering – Mechanical Engineering Department – Parit Raja – Johor – Malaysia.
2. Universiti Tun Hussein Onn Malaysia – Faculty of Mechanical and Manufacturing Engineering – Aeronautical Engineering Department – Parit Raja – Johor – Malaysia.
3. Universiti Tun Hussein Onn Malaysia – Faculty of Electrical and Electronic Engineering – Electrical Engineering Department – Parit Raja – Johor – Malaysia.

***Corresponding author:** safyanu@uthm.edu.my

ABSTRACT

The paper focuses on optimizing the power device sizing of a solar aircraft with the goal of reducing its overall mass and improving flight duration through the application of a multidisciplinary design optimization framework. The paper is organized into design strategy and optimization phases. The design strategy, mission specifications, and performance requirements were defined, and, using data from the photovoltaic geographical information system, a Malaysian solar radiation model was developed to enhance the accuracy of solar energy predictions. Performance analysis of selected airfoils was conducted, and the WE-3.55 airfoil exhibited the best characteristics. The airfoil was selected as the most suitable for the aircraft configuration. The optimization phase employed ModeFrontier software to optimize the solar aircraft sizing, minimize structural mass, and prolong flight endurance. The optimal results revealed an available solar energy of 283.56 Wh against a required electrical energy of the solar aircraft of 228.2 Wh, with a solar cell area of 0.57 m^2 and a total aircraft mass of 2.05 kg. The final configuration requires 16 solar cells (0.580 V, 6.01 A) and 36 battery units (2.15 V, 2.5 Ah). Compared to previous designs, the optimization of the power device provides reductions of 50% in solar cells, 48.57% in battery units, 25.81% in total mass, and a 3.7% increase in flight time. These results validate the effectiveness of the multidisciplinary design optimization approach in improving the energy performance and overall efficiency of solar-powered aircraft.

Keywords: Solar aircraft; Solar radiation model; Aerodynamics analysis; Multidisciplinary optimization; Optimal design.

INTRODUCTION

The idea of applying solar energy to power aircraft has been explored for several decades. Early pioneering work by Boucher resulted in the development of Sunrise I and II in 1974 and 1975. Consequently, Dr. Paul MacCready advanced the field by constructing the first manned solar aircraft, the Gossamer Penguin, in 1980, followed by the Solar Challenger in 1983. Later developments, such as the Sky-Sailor in 2005 and the Solar Impulse I and II projects by Piccard and Borschberg, demonstrated significant progress in solar aircraft technology (Safyanu *et al.* 2018). These successes climax the steady evolution and innovation in solar-powered flight (Mastoras *et al.* 2023; Abdulrahman *et al.* 2025). In spite of the outstanding improvements, solar aircraft continue to encounter problems in harnessing and converting sustainable solar energy and storing adequate energy to extend flight duration (Safyanu *et al.* 2019; Danjuma, 2022). Attaining constant flight necessitates a careful balance between aircraft mass and the available power required to produce sufficient lift (Gao *et al.* 2015, Liu *et al.* 2025).

Received: May 25, 2025 | **Accepted:** Aug 8, 2026
Peer Review History: Single Blind Peer Review.
Section editor: Luiz Martins-Filho

CC BY

Multidisciplinary design optimization (MDO) offers an effective framework for solving complex, interdependent engineering problems by incorporating multiple analytical domains (Hosseini *et al*. 2016). The competitiveness of any engineering company determines the capability to develop successful engineering products (Papageorgiou *et al*. 2018). MDO has proven to be a game-changer in the aerospace sector, where design complexity and competition are high. It offers a comprehensive approach for improving design efficiency and providing strategic advantages (Nguyen *et al*. 2013). The effectiveness of MDO in solar aircraft applications is supported by statistical evidence, particularly in integrated tool deployment, disciplinary modeling, and analysis capability (Papageorgiou *et al*. 2018). The applicability of optimization algorithms with previous studies, such as the single-objective student psychology-based optimization algorithm, solve complex multi-objective scheduling problems in satellite systems (Jia & Yu 2025).

Recent research on MDO has conventionally highlighted enhancing the flight performance by optimization of aerodynamics, mass distribution, thrust, and energy management. Typical objectives include reducing total aircraft mass and power requirements while maximizing available power (Papageorgiou *et al*. 2018). Almost all recent review studies buttress the above statements. The statements above are supported by recent studies. The aim of proposing a new analytical mass model is to optimize the cruise speed and lift coefficient of a unmanned aerial vehicle (UAV), thereby reducing the fixed load of total mass (Montagnier and Bovet 2010).

Ayele *et al*. (2013) demonstrated that composite materials and energy–requirement balancing can minimize wing mass and reduce night-time altitude loss, overall weight, and payload mass. Additional research has incorporated structural strength, aerodynamic efficiency, and material properties into MDO frameworks to reduce mass and enhance power performance. The total mass, structure, strength, aerodynamics, and other structures are incorporated into the MDO tool. The objectives are to reduce mass and power enhancement (Mattos *et al*. 2013).

Further studies evaluating aerodynamic, structural, and stability parameters have achieved improvements in lift generation, drag reduction, and overall weight minimization (Vieira *et al*. 2013, Adler and Martins 2023). Energy limitations and structural trade-offs have also been analysed to lower total mass (Zhang *et al*. 2017). Comparative assessments of multi-objective optimization strategies for medium-altitude long-endurance UAVs have emphazised the importance of mission requirements, core subsystem characteristics, and energy storage design, with goals including improved electric endurance, reduced hybrid-system volume, lower energy consumption, and shorter runway requirements (Donateo *et al*. 2018, Sun *et al*. 2025). Other advancements include enhanced solar energy storage and reduced tracking error using the adaptive Lyapunov guidance vector field within a fluid dynamics framework (Wei *et al*. 2020, Ismail *et al*. 2026). Additionally, solar aircraft size and cruise speed have been optimised using genetic algorithms (Shiau *et al*. 2010).

In this study, a Malaysian solar radiation model (MSRM) and mission specification path were developed for solar aircraft operation. Furthermore, an MDO tool was employed to improve power device sizing, thereby reducing aircraft mass and extending airborne duration. The main objectives of this paper were to enhance flight duration and reduce total aircraft mass by optimizing the power device configuration using ModeFrontier, a commercial MDO software platform.

METHOD

The methodology created an integrated aircraft design framework and optimization framework for determining the effective power-system concept of an solar powered aircraft (SPA) while simultaneously reducing aircraft mass and prolonging flight endurance. The framework compares five inter-related disciplines:

- Solar-resource modeling;
- Aerodynamic analysis;
- Aircraft mass estimation;
- Electrical power and energy-system sizing;
- Multidisciplinary optimization.

In the aircraft design strategy, as shown in Fig. 1, the MSRM is developed from solar resource data obtained from photovoltaic geographic information system (PVGIS), followed by defining the aircraft mission profile, energy balance, aerodynamic analysis,

aircraft mass estimation, and energy and mass balance. The aerodynamic and energy requirements are subsequently used to determine the photovoltaic (PV) and battery requirements. In the optimization strategy, the major aircraft and power-system design parameters are varied within prescribed limits using ModeFRONTIER and the multi-objective genetic algorithm II (MOGA-II), as depicted in Fig. 2.

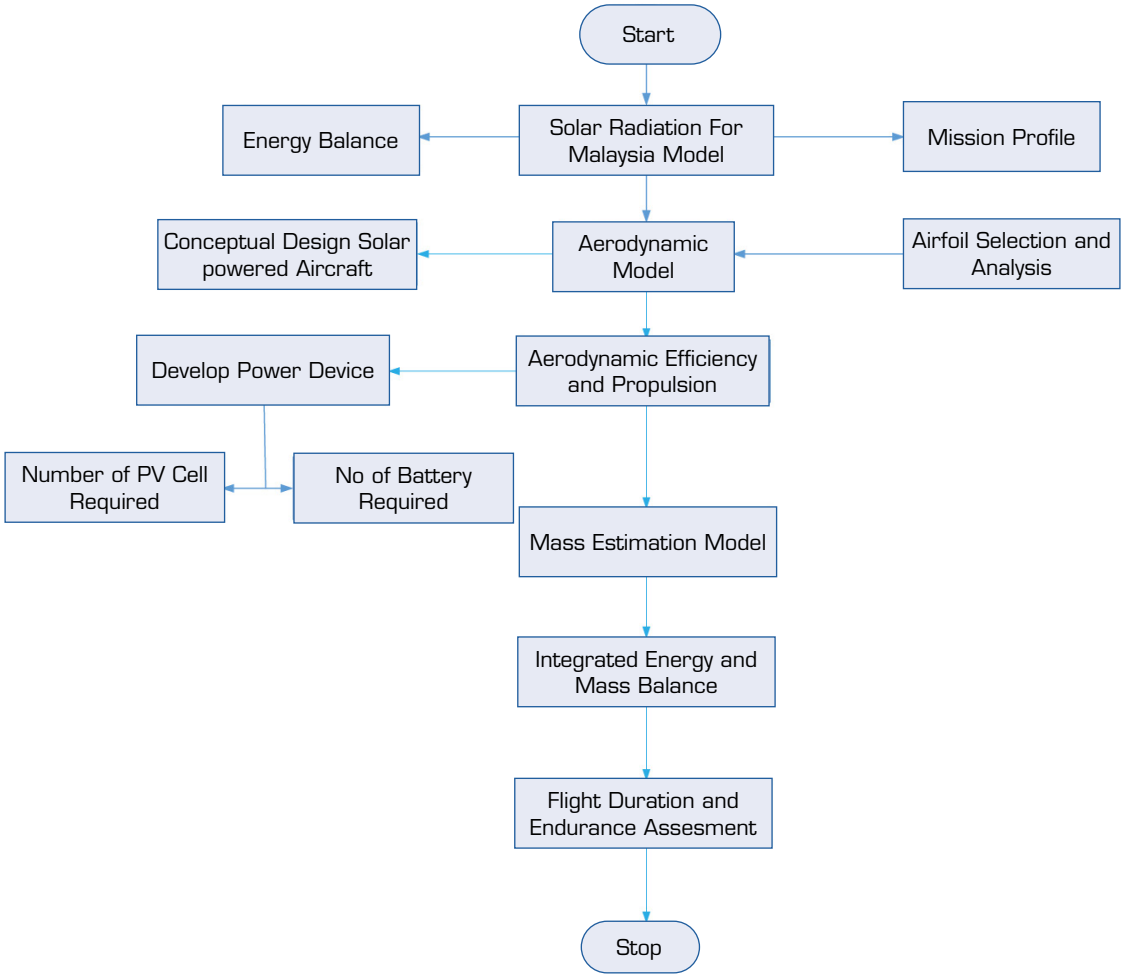

PV: photovoltaic.

Figure 1. Aircraft design strategy.

Malaysia solar radiation model

The MSRM was designed using PVGIS software, which provides radiation data for different regions of the globe. Figure 3 shows the PVGIS window. Radiation data for Malaysia were collated over five years using PVGIS, and MSRM was formulated using the sixth-order polynomial. The daily solar energy per square meter can be easily calculated using Eq. 1. The maximum irradiance and the period of solar radiation (T_{day}) are obtained from the PVGIS.

$$E_{day\ density} = \frac{I_{max} T_{day}}{\pi/2}\ \eta_{wthr} \tag{1}$$

Where: $E_{day\ density}$: the daily solar energy per square meter; I_{max}: maximum irradiance; T_{day}: time of the day; η_{wthr}: weather efficiency.

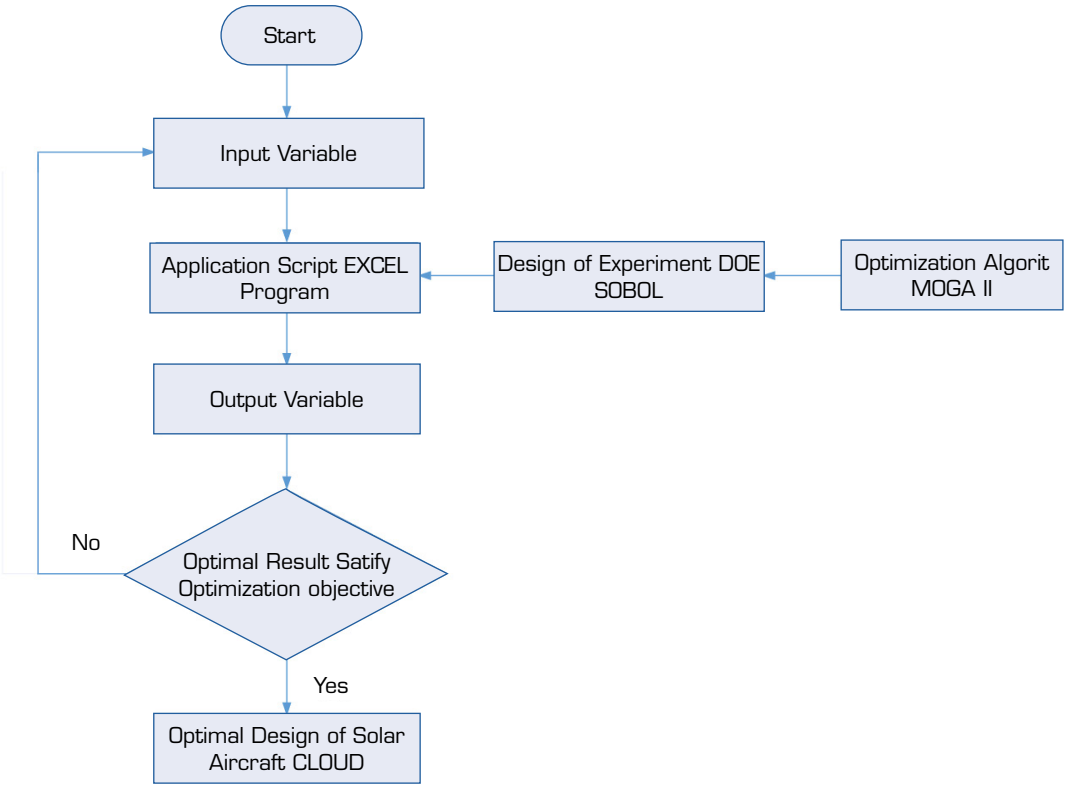

DOE: design of experiment; SOBOL: Sobol sequence; MOGA-II: multi-objective genetic algorithm II.

Figure 2. Optimization strategy.

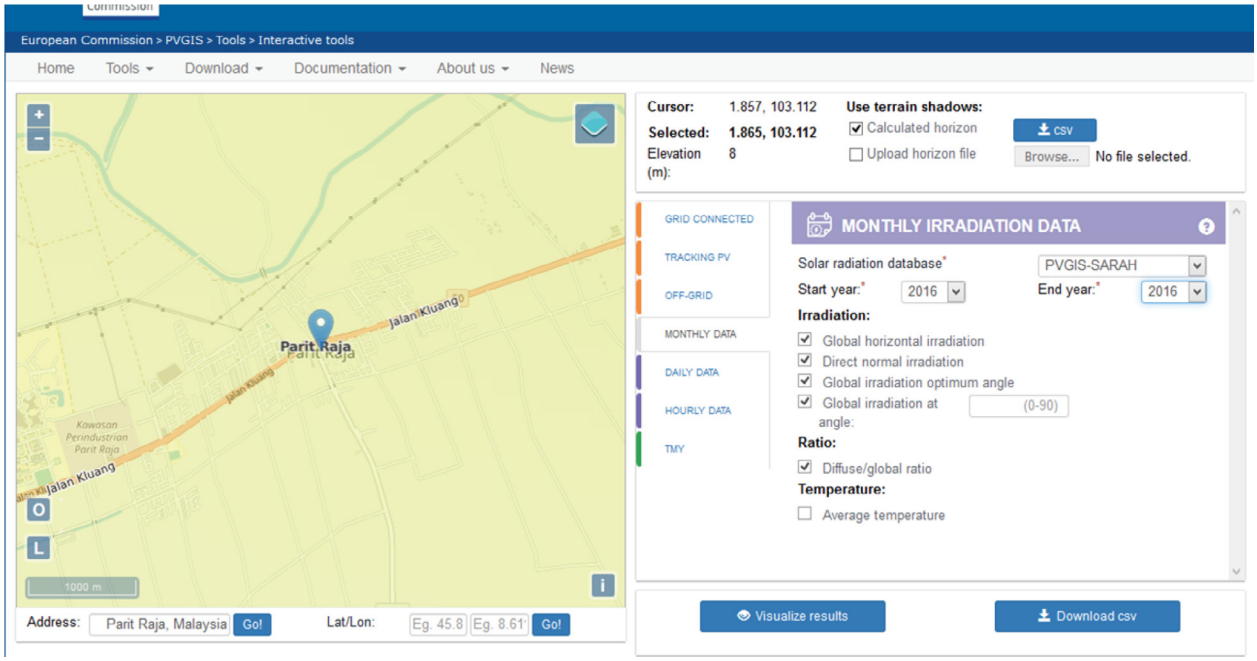

Figure 3. Photovoltaic geographic information system window.

Mission profile

The mission profile/specification is a flight-path design that guides the aircraft operations for 48 hours. The aircraft is launched at sunrise, when solar energy is available for the climb stage and cruise to a higher altitude. The aircraft descended at sunset to a lower altitude, and it maintains a lower altitude to conserve energy. The next day, at sunrise, it climbs to a higher altitude. Then, it descends to the ground as the mission is complete.

Airfoil selection and low-Reynolds-number aerodynamic analysis

Five airfoils were selected for the analysis, namely:

- AQUILA 9.3% (Reddy *et al.* 2016);
- LA2573A (Najafi 2001);
- S9000 (9%) (Najafi 2001);
- S9037 (9%) (Hartney, 2011);
- WE-3.55 (Noth *et al.* 2006).

XFLR5 v6 software was used for airfoil analysis at a Reynolds number 500,000 and a 4 angle of attack. The goal is to identify the optimal among them and obtain an efficient and robust wing configuration.

The airfoils are analyzed under low-Reynolds-number operating conditions of the SPA configuration. The airfoil aerodynamic parameters consist of the lift coefficient (C_L), drag coefficient (C_D), and lift-to-drag ratio (C_L/C_D).

XFLR5 is an aerodynamic analysis tool that employs panel-method formulation integrated with viscous boundary-layer analysis through XFOIL program and is not a full computational fluid dynamics (CFD) solver. Therefore, its limitations are flow separation, post-stall behaviour, three-dimensional wing effects, and other complex viscous phenomena, which are considered when interpreting the aerodynamic results.

Aircraft aerodynamic model

The aerodynamic characteristics are integrated into the conceptual aircraft model after selecting the airfoil. During steady level flight, the lift generated by the wing must balance the aircraft's weight. It is important because the aircraft drag does not represent the complete two-dimensional airfoil drag obtained from XFLR5. Therefore, before calculating the propulsion power requirement, the induced and parasitic drag are incorporated into the aircraft-level model.

On the wing, the air experiences laminar flow at constant speed , while on the upper and lower surfaces, pressure is produced. As a result, lift and drag forces are created.

Using Eqs. 2 and 3, lift and drag forces can be calculated:

$$W = mg = F_L = C_L \frac{\rho}{2} S v^2 \tag{2}$$

$$T = F_D = C_D \frac{\rho}{2} S v^2 \tag{3}$$

Where: C_L: lift coefficient; C_D: drag coefficient; ρ: air density; S: wing area; v: the relative speed of the aircraft.

If the wind is assumed negligible, the relative speed equals the ground speed. The airfoil, the angle of attack α, and the Reynolds number Re are used to determine C_L and C_D, which is the function of airflow viscosity (Eq. 4):

$$Re = \frac{\rho v c}{\mu} = \frac{\mathrm{v c}}{\upsilon} \tag{4}$$

Where: μ: dynamic viscosity; v: kinematic viscosity; c: chord.

Induced drag is produced as a result of a vortex developed at the aircraft's wingtip. Induced drag is typically considered when aircraft have small aspect ratios. Also, the non-lifting parts, *e.g.*, tail and fuselage, experience parasitic drag. The final drag is the sum of all the drags, *i.e.*, C_D, as presented in Eq. 5:

$$C_{D\ ind} = \frac{{C_D}^2}{e\pi AR} \tag{5}$$

Where: *e*: Oswald efficiency factor.

The number varies from 0.7 to 0.85, but it is approximately between 0 and 1. In an ideal situation, the number is 1 when the load distribution is elliptical (Eq. 6).

$$C_D = C_{D\ afl} + C_{D\ ind} + C_{D\ par} \tag{6}$$

Where: $C_{D\ afl}$: airfoil drag; $C_{D\ ind}$: induced; $C_{D\ par}$: parasitic drag. *AR*: aspect ratio, *i.e.*, AR = b/c = b^2/(bc) = b^2/S

Aerodynamic efficiency and propulsion power

By combining the lift and drag relationships, the aerodynamic efficiency and the propulsion power establish the direct connection between airfoil selection and mechanical power for level flight. The required mechanical power can be expressed as a function of aircraft mass, wing area, air density, velocity, and aerodynamic coefficients.

Mechanical power for level flight

An aircraft experiences four forces acting on it: from the wing upward is the lift L, which equals the weight W. Also, from the rear, the drag D is equal to the thrust T from the forward at the propeller (Eq. 7):

$$P_{mech} = \frac{C_D}{{C_L}^{3/2}} \sqrt{\frac{(mg)^3}{S}} \sqrt{\frac{\rho}{2}} \tag{7}$$

The mechanical power for the level can be calculated using the Eq. 8:

$$P_{mech} = \frac{C_D}{{C_L}^{3/2}} \sqrt{\frac{2ARg^3}{\rho}} \frac{m_{tot}^{3/2}}{b} \tag{8}$$

Electrical power for flight

The efficiencies of the motor, motor controller, gearbox, and propeller are integrated to calculate the electrical power required by the propulsion system (Eq. 9):

$$P_{Eflight} = P_{mech} \frac{1}{\eta_{mot}\,\eta_{ctrl}\,\eta_{grb}\,\eta_{plr}} \tag{9}$$

Where: P_{mech}: mechanical power; η_{mot}: the efficiency of the motor; η_{ctrl}: motor controller; η_{grb}: gearbox; η_{plr}: propeller.

The aerodynamic optimization and solar power sizing are link together. They also produce an airfoil or wing configuration that produces lower drag that requires lower mechanical power and, consequently, lower electrical power. Minimizing the required PV generation and battery storage capacity reduces the aircraft mass and potentially further reduces the required propulsion power.

Total electrical power requirement

The total electrical power demand comprises battery elimination circuit (BEC), propulsion, avionics, and payload requirements. The total electrical power is subsequently used to determine the daily energy consumption and the required PV and battery capacities (Eq. 10):

$$P_{elec\ tot} = P_{Eflight} + \frac{1}{\eta bec}(P_{av} + P_{pld}) \tag{10}$$

Where: $P_{Eflight}$: electrical power; P_{av}: avionics power; P_{pld}: payload power; ηbec: BEC efficiency.

BEC is a concept that regulates an unstable high-voltage input to a more stable lower-voltage output. This avoids the use of separate batteries for subsystems. BEC is used in embedded systems, UAVs, and automotive electronics. These eliminate the need for multiple batteries, reduce the weight, improve energy efficiency, simplify maintenance, and improve reliability.

Energy consumption

The daily electrical energy requirement is computed by inputing the daylight and nighttime operating periods and the charging and discharging efficiencies of the battery (Eq. 11):

$$E_{elec\ tot} = P_{elec\ tot}\ (T_{day} + \frac{T_{night}}{\eta chrg\ \eta dchrg}) \tag{11}$$

Where: $P_{elec\ tot}$: total electrical power; $\eta chrg$: charge efficiency; $\eta dchrg$: discharge efficiency of the battery for the night period; T_{night}: night duration; T_{day}: the day duration

Subsequently, the energy requirement is used as an input to the PV and battery sizing models.

Photovoltaic solar-cell sizing

The required solar-cell area is determined from the total electrical power demand, solar-cell efficiency, maximum power point tracker (MPPT) efficiency, weather efficiency, daylight duration, and battery charging/discharging efficiencies. Hence, the PV system is sized to provide sufficient energy to operate the aircraft during daylight and recharge the battery for nighttime operation.

The solar-cell area is expressed as Eq. 12:

$$A_{sc} = P_{Etot}\ \frac{\pi}{2\eta_{sc}\ \eta_{cbr}\ \eta_{mppt}\ \eta_{wthr}} \left(1 + \frac{T_{night}}{T_{day}}\ \frac{1}{\eta_{chrg}\eta_{dchrg}}\right) \frac{1}{I_{max}} \tag{12}$$

Where: P_{Etot}: total electrical power; η_{sc}: cell efficiency; η_{mppt}: MPPT efficiency; η_{wthr}: efficiency of the solar cell in different weather conditions; T_{day}: length of the day; T_{night}: length of the night; η_{chrg}: charging efficiency; η_{dchrg}: discharging efficiency; I_{max}: maximum irradiance; η_{cbr}: cambered efficiency.

Camber efficiency in the context of UAV applications is the enhancement of aerodynamic performance resulting from airfoil curvature. It can be expressed as a ratio of aerodynamic coefficients.

CC BY

Battery sizing

The battery mass is determined from the nighttime duration, battery discharge efficiency, battery-specific mass coefficient, and total electrical power (Eq. 13):

$$m_{bat} = \frac{T_{night}}{\eta_{dchrg}\ k_{bat}} P_{elec\ tot} \tag{13}$$

Where: T_{night}: length of the night; η_{dchrg}: battery discharge efficiency; k_{bat}: overall mass coefficient for batteries; $P_{elec\ tot}$: total electrical power.

The battery is sized to supply the aircraft during periods when solar radiation is unavailable, particularly during the nighttime portion of the mission. The number of battery units is determined from the required energy storage capacity and the rated energy capacity of the selected battery unit. The battery-sizing procedure is coupled to the aerodynamic model because increased in drag increases propulsion power, which increases nighttime and daily energy demand and consequently the required battery capacity.

Mass estimation model

The aircraft mass is estimated using the mass-estimation approach developed by Andre Noth and Roland Siegwart (2006), which calculates the masses of individual components. The total aircraft mass consists of the fixed masses, airframe structure, solar cells, MPPT system, battery, propulsion system, payload, and avionics. The mass model is iteratively updated during optimization because the aircraft mass affects lift requirements and consequently aerodynamic drag and propulsion power.

A comprehensive mass model is essential for determining the individual mass of the constituent components of the solar aircraft. However, the total mass (m_{tot}) is predetermined and can be used to calculate the mechanical power for level flight (P_{mech}) using Eq. 8. Subsequently, the masses of the aircraft's various components are calculated.

Fixed masses

The fixed mass of an aircraft is the combined mass of the components that are assumed to be constant for the entire optimization process. The components are always fixed, not affected by any aerodynamic changes or any energy system design variable, as shown in Eq. 14:

$$m_f = m_{av} + m_{pld} \tag{14}$$

Where: m_{pld}: payload mass; m_{av}: avionics mass; m_f: fixed mass.

Airframe structure mass

Airframe structure mass is the mass that provides the required strength, stiffness, and aerodynamic shape while supporting the aircraft's operational loads, as shown in Eq. 15:

$$m_{af} = k_{af} AR^{x_2} b^{x_1} \tag{15}$$

Where: x_1: structural mass area exponent; x_2: structural mass aspect ratio exponent; k_{af}: the structural mass constant; AR: aspect ratio; b = wingspan.

Mass of the propulsion group

Mass of the propulsion is the combined mass of the components that convert electrical energy into mechanical thrust, as shown in Eq. 16:

$$m_{prop} = k_{prop} P_{Eflight} \tag{16}$$

Where: $P_{Eflight}$: electrical power available to sustain flight; k_{prop}: mass coefficient for the propulsion group.

Mass of the solar cell

Mass of the solar cell is the total mass of the PV cells installed on the wing or any available surface of the aircraft for the conversion of solar energy to electrical energy, as shown in Eq. 17:

$$m_{sc} = (k_{sc} + k_{enc}) A_{sc} \tag{17}$$

Where: A_{sc}: area of solar cells; k_{sc}: solar cell mass per unit area; k_{enc}: mass of enclosure and encapsulation.

Mass of the maximum power point tracker

The mass of the MPPT is the mass of the electronic power device that continuously regulates the operating point of the PV system to its maximum power output, as shown in Eq. 18:

$$m_{mppt} = k_{mppt} \times I_{max} \times \eta_{sc} \times \eta_{cbr} \times \eta_{mppt} \times A_{sc} \tag{18}$$

k_{mppt}: MPPT coefficient; I_{max}: maximum irradiance; cells η_{sc}: efficiencies of the solar; η_{cbr}: curvature of the solar cells; η_{mppt}: MPPT efficiency.

Integrated energy and mass balance

The integrated energy and mass balance is used to ensure consistency between aircraft mass, aerodynamic performance, power consumption, and energy-system sizing. The calculation was performed in Microsoft Excel to determine the aircraft mass and energy-system requirements. The calculation process ensures that the PV and battery systems are not sized independently of aircraft aerodynamic performance, as shown in Fig. 4. The process is integrated into the MDO to achieve the optimal design.

Flight duration and endurance assessment

The flight duration is evaluated based on the relationship between the available solar energy, stored battery energy, and total aircraft energy consumption. The resulting flight duration is evaluated using the mission energy balance, with particular attention to the aircraft's ability to maintain flight throughout the nighttime period. The optimization produced a structure that decreases power demand and total mass of the system while upholding sufficient energy availability for the set mission duration.

Multidisciplinary optimization framework

The optimization is performed using ModeFRONTIER. The optimization framework sets the design variables with limits, objectives, and constraints to achieve the design output (optimal design). The optimization problem is analyzing the design variables, the objective function/output, and the design constraints.

CC BY

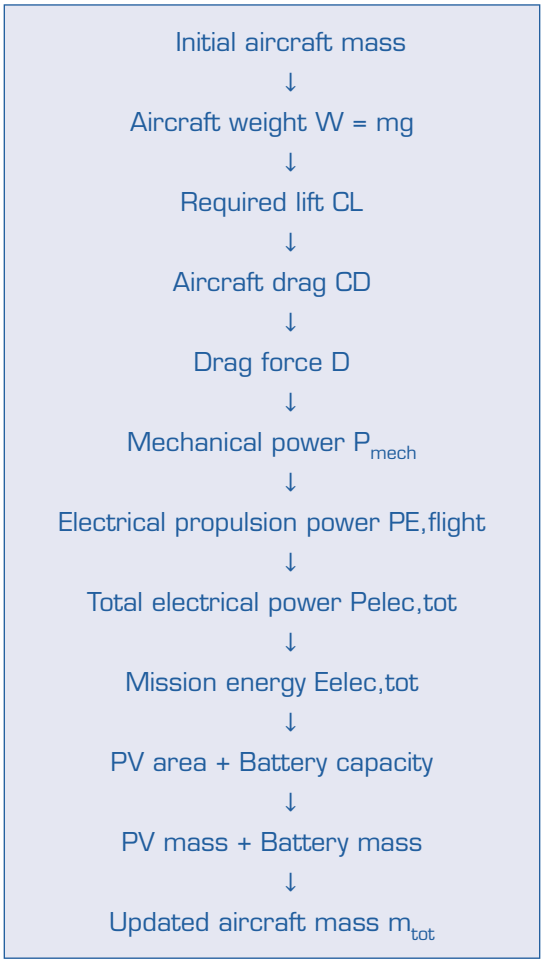

Figure 4. Integrated energy and mass balance process.

Optimization variable

- Wingspan;
- Wing chord;
- Aircraft mass;
- Solar radiation;
- Aircraft velocity;
- Lift coefficient;
- Drag coefficient.

Optimization output variable

- Daily solar energy;
- Total electrical energy;
- Aircraft total mass.

Optimization objectives

- The minimization of the total mass of aircraft;
- The maximization of daily solar energy (flight endurance);
- The minimization of total electrical energy.

Optimization constraints

- Minimize the total mass to less than 2.5 kg;
- Minimize total electrical energy to less than 500 Wh.

Optimization with ModeFrontier software

ModeFrontier is a comprehensive package for computerizing and optimizing the design process. The software provides an avenue to reduce complexity, improve efficiency, and reduce process time. The software is categorized into workflow editor, design space, and run analysis. The workflow editor consists of problem definition (input, output, optimization objectives, and optimization constraints), the definition of the design of experiment (DOE), and the definition of the optimization strategy. The design space supports data analysis, visualization, metamodel, and the run analysis evaluates the design.

Workflow creation

The workflow setup includes all the defined entities involved: input variable, output variable, design objective, and design constraints. The application script (Microsoft Excel) is used to calculate mathematical expressions. The data flow is set from input to output, and the optimization strategy is set to have the logic flow.

The data flow sets the input variable's lower and upper bounds and defines constants. The design objective and the constraints are set, and the input variables are achieved, as shown in Table 1. The DOE setup, the space filler in the design of experiments, is based on a pseudo-random Sobol sequence, which works with two to 20 variables. The designs are uniformly distributed in the design space. The number of generated designs is limited to 256,000. On the design table, the Sobol sequence algorithm generated 20 designs. The MOGA-II is used to solve the design problem in the optimization algorithm setup. The MOGA-II is designed for fast Pareto convergence. The population size of MOGA-II corresponds to the size of the DOE dataset. The algorithm configuration is self-initializing, and the number of evolution generations is 500.

Table 1. Optimization variables.

Variable	Lower bound	Upper bound
Wingspan (b)	3	3.5 m
Chord (a)	0.25 m	0.3 m
Mass (m)	2 kg	5 kg
Radiation (H)	750	825
Lift coefficient (constant)	0.913	0.913
Drag coefficient	0.03	0.06
Velocity (m/s)	7	10

RESULTS AND DISCUSSION

Malaysia solar radiation model

A developed MSRM, constructed using a sixth-order polynomial, was validated against experimental solar radiation measurements as shown in Fig. 5. The evaluation shows that measured data are slightly lower than the predicted data but follow the same trend throughout the diurnal cycle. The high coefficient of determination ($R^2 = 0.998$) supports the model, indicating that it reliably represents solar radiation behaviour under Malaysian environmental conditions.

Global solar radiation is shown by the thin blue lines; diffuse and direct radiation is shown by the brown lines; and the predicted MSRM output is the yellow dotted lines. The model displayed the natural phenomenon of the rise and fall of solar irradiance during the daytime and validated a strong correlation with actual field data. The predicted maximum irradiance, and the total duration of effective daily solar radiation (T_day) are I_max = 825 W/m^2 and 12 hours, respectively. The values are consistent with typical tropical solar patterns.

CC BY

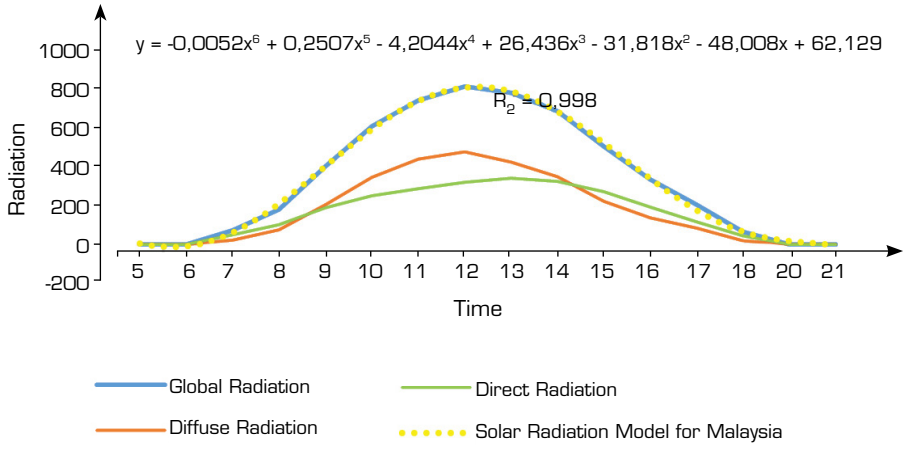

Figure 5. Malaysia solar radiation model (Wh/m^2).

Consequently, the MSRM provides a reliable and accurate model for designing SPA energy prediction, power system sizing, and optimization analyses.

Malaysia energy balance

The MSRM model was used to develop the Malaysian energy balance based on the maximum irradiance (I_{max}) obtained as shown in Fig. 6. The energy balance shows that the solar energy acquired over 12 hours is 540.96 Wh. Table 2 depicts a total electrical power requirement of 18 W. The energy generated powers the solar aircraft, and the excess is stored in the rechargeable batteries. Therefore, the energy balance confirms that the generated solar energy is sufficient to power solar aircraft during the day and store the excess in a battery to sustain the operation at night. Overall, the solar energy cycle is designed to support a long endurance mission lasting up to 48 hours nonstop.

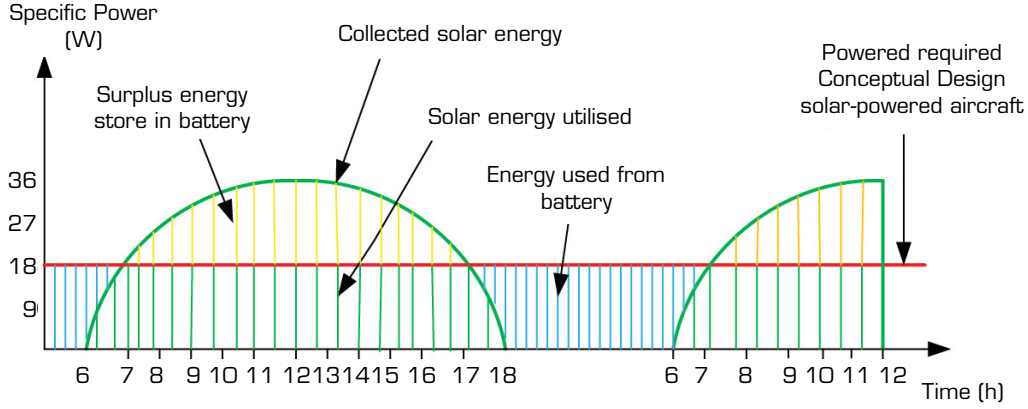

Figure 6. Solar energy balance for Malaysia.

Table 2. Aircraft total electrical power requirement.

S/N	Input data		Output data	
1	Aircraft power	15.07 W	Total electrical power	18 W
2	Payload power	1.5 W		
3	Avionic power	0.5 W		
4	BEC efficiency	65%		

In addition, the available solar energy for the period of 12 hours is the dense green lines; the aircraft's total electrical requirement is the red horizontal line; the solar energy utilized during daytime is the thin green lines; the surplus energy that is stored in the battery is the thin yellow lines, and the energy drawn from the battery is the thin blues lines.

In general, the energy balance diagram validate the system can sustain long endurance mission efficiently under Malaysian solar conditions from solar energy acquired, utilization, and storage processes.

Mission path

The mission path is developed based on the solar balance for Malaysia with specifications for airbone nonstop operation for 48 hours. As depicted in Fig. 7, the path comprises three phases: the climb and cruise during daytime and the descent during nighttime. At initial take-off, the aircraft climbs to an altitude between 300 and 500 m. Then, from 7 a.m. to 6 p.m., the aircraft reaches its cruise altitude while solar energy is available. At this altitude, the aircraft duel constantly, and the solar energy system meets both the propulsion demand and the on-board battery bank for night operations.

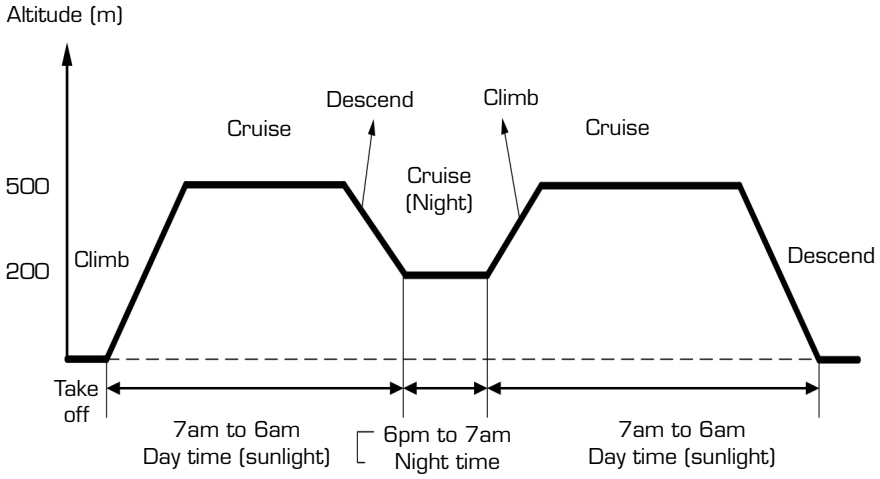

Figure 7. Optimal design of solar-powered aircraft.

The aircraft descends to a lower altitude toward 6 p.m. as the sun sets, then cruises at night. The altitude is reduced to meet the demands of aerodynamic drag, induced power, and total energy consumption as the aircraft is solely dependent on the stored energy from the rechargeable battery. The night phase cruise showcases the optimization of the systems required to provide a lower altitude and energy conservation to sustain flight endurance at night.

On the second day, at sunrise (7 a.m.), the solar energy is available, and the operation continues, powering the aircraft and storing the excess in the battery bank. The operation reveals the aircraft's capability to operate at varying altitudes and times of day. Then, the final descent for landing concludes the mission profile.

In general, the mission profile proves the importance of altitude modulation as a harmonizing tool between the power generation and energy utilization. The adoption of a mission profile enables long-endurance flight and leverages the efficacy of rechargeable batteries in energy management to sustain flight operation for 48 hours. The altitudes of 500 and 200 m were carefully selected from previous studies with similar configurations (Danjuma *et al.* 2021).

Airfoil analysis results

The aerodynamic analysis of five selected airfoils was evaluated at a Reynolds number of 500,000 and a 4° angle of attack, as shown in Table 3. The selection criteria were a high lift coefficient, low drag coefficient, and high lift-to-drag ratio, according to Reddy *et al.* (2016). The aerodynamic properties are important in solar aircraft, influencing aerodynamic efficiency of lift generation, energy consumption, and overall flight endurance.

CC BY

Table 3. The aerodynamic characterization and comparisons of the airfoils*.

Airfoil	AQUILA-9.3%	LA2573A	S9000 (9%)	S9037 (9%)	WE-3.55
Thickness (%)	9.3	13.70	9.01	9.00	9.30
Max camber (%)	4.05	3.19	2.37	3.49	3.55
C_L	0.833	0.630	0.757	0.828	0.913
C_D	0.008	0.012	0.008	0.008	0.008
C_L/C_D	101.911	53.004	93.235	104.897	117.248
No. of panels	69	101	121	121	117

*At 5.0 x 10^5 Reynolds number and 4° angle of attack.

The WE-3.55 exhibits most favorable aerodynamic characteristics; C_L = 0.913, C_D = 0.008, and CL/CD = 117.248. The airfoil showcases a superior efficiency in producing lift and maintaining minimal drag. The efficiency directly improves the performance of solar aircraft in power usage and long endurance flight.

Other airfoils exhibit moderate performance, such as AQUILA-9.3% and S9037 (9%), with CL/CD = 101.911 and 104.897, respectively. In addition, airfoils LA2573A and S9000 (9%) also have a lower CL/CD. However, these remain lower than that of the WE-3.55 airfoil.

Based on the superior aerodynamic characteristics of WE-3.55, it is selected as the optimal airfoil for wing design, while NACA 0008 airfol is chosen for the tail and rudder surface design in accordance with Raymer (2007), standard design recommendations, as it provides balanced aerodynamic stability without contributing additional pitching moments.

In general, the selection of appropriate airfoil in solar aircraft design translates to high aerodynamic efficiency, which is essential for efficient performance and long-endurance mission.

Conceptual design of solar-powered aircraft

Table 4 shows the key input and output variables used in the conceptual design of the SPA, computed using Microsoft Excel. The design employed geometric and aerodynamic parameters, with the energy requirements for long-endurance airborne.

Table 4. Summary of conceptual design of solar-powered aircraft (MS-Excel).

Input variable			Output variable		
Parameter	**Value**	**Units**	**Parameter**	**Value**	**Units**
Mass	3	Kg	Mechanical power	10.03	W
Wing Span	3.2	m	Total electrical power	18.35	W
Chord	0.3	m	Total electrical energy	435.48	Wh
Radiation	825	W/m^2	Daily solar energy	540.96	Wh
Aspect ratio	11.25	-	Solar cell area	0.58	m^2
Lift coefficient	0.913	-	Total wattage	108.87	W
Drag coefficient	0.041	-	Quantity of solar cell	32	-
Daytime	12	hrs	Quantity of battery	70	-
Nighttime	12	hrs	Total mass	2.76	kg

The SPA geometric configuration is defined by an aspect ratio of 11.25, a wingspan of 3.2 m, and a total aircraft mass of 3 kg. The wing planform includes a 7° polyhedral angle, with a tapered profile that reduces from 0.3 m at the root chord to 0.2 m at the tip chord along a 0.5-m semi-span. These geometric variables, specifically the aspect ratio and wingspan, serve as the primary inputs for generating the wing profile in XFLR5 v6 using the previously selected high-efficiency airfoil, WE-3.55.

The aerodynamic coefficients used for performance estimation include C_L of 0.913 and C_D of 0.041, defined under the expected flight conditions. The radiation input, based on maximum Malaysian solar irradiance, is 825 W/m^2, with equal daytime and nighttime durations of 12 hours each, aligning with the solar radiation model.

The calculated output parameters determine the aircraft's power and energy characteristics. The mechanical power required for flight is 10.03 W, while the total electrical power needed, including payload and avionics, amounts to 18.35 W. The corresponding total electrical energy consumption is 435.48 Wh, compared to a daily available solar energy of 540.96 Wh, indicating sufficient solar energy to meet operational demands. The required solar cell area is 0.58 m^2, producing a total power of 108.87 W at peak irradiance.

The design specifies 32 solar cells and 70 battery units, which together reduce the final aircraft mass of 2.76 kg before optimization, to support the energy requirement. The reduction in mass proves the goal of improving flight performance through efficient weight and energy management.

In general, Table 4 demonstrates a balanced design that integrates aerodynamic efficiency, efficient solar energy utilization, and lightweight structural considerations, providing a foundation for subsequent optimisation and performance analyses.

Optimal design of solar-powered aircraft

The optimal design variables for the SPA were obtained using the ModeFrontier optimization platform with the MOGA-II evolutionary algorithm, as shown in Table 5. The optimization process aimed to achieve three primary objectives:

Table 5. Summary of the optimal design (ID 4710).

Input variable		Output variable	
Chord	0.28 m	Daily solar energy	283.56 Wh
Drag coefficient	0.031	Total electrical energy	228.32 Wh
Lift coefficient	0.913	Quantity of solar cell	16
Radiation	825 W/m^2	Quantity of battery	36
Velocity	7.64 m/s	Total mass	2.05 kg
Wingspan	3.3 m		
Mass	2.76 kg		

- Maximize daily solar energy generation;
- Minimize total electrical energy required for flight;
- Minimize the overall mass of the aircraft.

The final mass and the conceptual design parameters from Table 4 served as the input variables for this optimization workflow.

Key optimal input parameters include a wing chord of 0.28 m, a CL of 0.913, a reduced CD of 0.031, and a wingspan of 3.3 m. The operational velocity is 7.64 m/s, and the solar irradiance remains fixed at 825 W/m^2, in accordance with the MSRM. These refined parameters collectively improve the aircraft's aerodynamic profile and energy efficiency, ensuring it meets its performance and endurance targets.

The optimal solution indicates a daily solar energy availability of 283.56 Wh, which satisfies the requirement for sustained daytime operation. Simultaneously, the total electrical energy required by the aircraft is significantly reduced to 228.32 Wh, indicating a well-balanced energy budget that supports long-endurance flight while maintaining sufficient reserves for system functionality. The optimization also yields a reduced aircraft total mass (including payload) to 2.05 kg, demonstrating substantial mass savings compared to the initial conceptual design mass of 2.76 kg.

The reduced mass, lower energy consumption, and sufficient solar energy availability all contribute to an enhanced system-level performance. The optimal configuration was subsequently employed to develop the final solar aircraft design, depicted in Fig. 8. Also, the summary of the conceptual and optimal designs with their percentage deviations is presented in Table 6, which further demonstrates the improvement in solar aircraft design for sustaining long endurance flight.

In general, the optimal results validates that the optimization objectives have been achieved.

CC BY

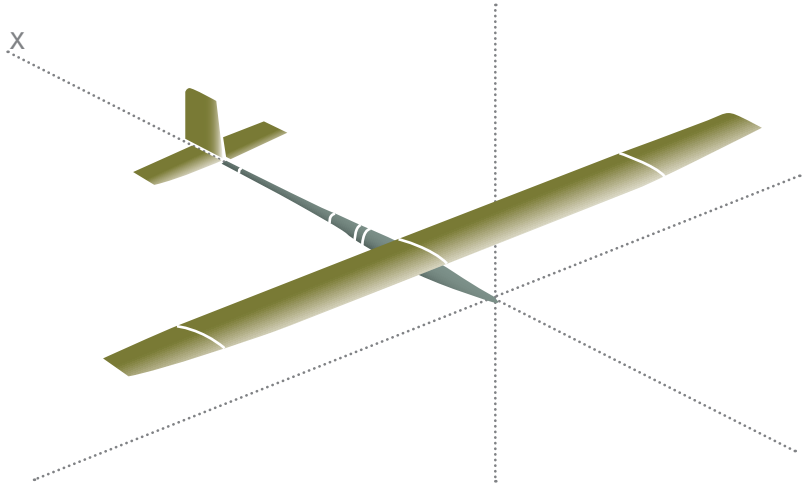

Figure 8. Optimal design of solar-powered aircraft.

Table 6. Summary of conceptual and optimal design with deviation.

Parameters	Conceptual design	Optimal design	Deviation (%)
Total electrical energy	435.48 Wh	228.32 Wh	47.57
Daily solar energy	540.96 Wh	283.56 Wh	47.58
Quantity of solar cell	32	16	50
Quantity of battery	70	36	48.57
Total mass	2.76 kg	2.05 kg	25.81

CONCLUSION

An MDO concept was integrated into the SPA design to improve power device sizing, reduce overall mass, and prolong flight endurance. In the design strategy, a comprehensive mission specification was determined to establish operational requirements and daily flight procedures. The MSRM and the corresponding energy balance were developed using PVGIS data to ensure accurate estimation and utilization of locally available solar energy resources. Aerodynamic analysis was performed on five selected airfoils, with the WE-3.55 airfoil being identified as the most efficient and subsequently adopted for the wing configuration.

The optimization process focused on reducing total electrical energy consumption, minimizing aircraft mass, and lowering solar energy demand. The MDO approach adopted ModeFrontier with the MOGA-II algorithm; the optimal design, ID 4710, yielded a total electrical energy requirement of 228.32 Wh, a daily solar energy availability of 283.56 Wh, and a total mass of 2.05 kg. The resulting configuration requires 16 solar cells and 36 battery units, representing reductions of 53% in solar cells, 51% in batteries, and 26% in aircraft mass compared to the initial design. Additionally, the airborne endurance improved by 3.7%, confirming the effectiveness of the optimization strategy.

CONFLICT OF INTEREST

Nothing to declare.

DATA AVAILABILITY STATEMENT

All data sets were generated or analyzed in the current study.

AUTHORS' CONTRIBUTION

Conceptualization: Safyanu B.D.; **Formal Analysis:** Safyanu B.D.; **Investigation:** Safyanu B.D.; **Resources:** Omar Z.B.; **Supervision:** Omar Z.B.; **Validation:** Abdullah M.N.; **Data curation:** Abdullah M.N.; **Writing – original draft:** Safyanu B.D.; **Writing – review and editing:** Abdullah M.N.; Safyanu B.D.; **Final approval:** Omar Z.B.;

FUNDING

Universiti Tun Hussein Onn Malaysia
Grant no: E15216

DECLARATION OF USE OF ARTIFICIAL INTELLIGENCE TOOLS

Generative artificial intelligence (AI) tools were used solely for grammar checking, language polishing, formatting consistency, and assistance in generating a conceptual schematic illustration during manuscript preparation. The AI-assisted illustration was reviewed and verified by the authors to ensure consistency with the physical configuration and numerical model presented in this study. All numerical simulations, optimization, calculations, data analysis, interpretation of results, and conclusions were performed and validated independently by the authors.

ACKNOWLEDGEMENTS

We would like to express our sincere appreciation to all the staff of the CFD Laboratory, Faculty of Mechanical and Manufacturing Engineering, Universiti Tun Hussein Onn Malaysia, for their kind gesture, support, and assistance. Their generosity and encouragement are deeply appreciated.

REFERENCES

Abdulrahman GAQ, Qasem NAA, Abdelrahman WG, Abdallah AM (2025) A review of powering unmanned aerial vehicles by clean and renewable energy technologies. Sustain Energy Technol Assess 73:104150. https://doi.org/10.1016/j.seta.2024.104150

Adler EJ, Martins JRRA (2023) Hydrogen powered aircraft Fundamental concepts key technologies and environmental impact. Progr Aerosp Sci 141:100922. https://doi.org/10.1016/j.paerosci.2023.100922

Ayele A, Gur O, Rosen A (2013) Conceptual multidisciplinary design optimization (MDO) of solar powered UAV. 53rd Israel Annual Conference on Aerospace Sciences. p. 731-750. https://cris.technion.ac.il/en/publications/conceptual-multidisciplinary-design-optimization-mdo-of-solar-pow/

Danjuma SB (2022) Aerodynamic design consideration for stability of a lightweight solar-powered aircraft. Path Sci 8(5):4010-6. https://doi.org/10.22178/pos.81-10

Danjuma SB, Omar Z, Abdullahi MN (2021) Design of power device sizing and integration for solar-powered aircraft application. J Mech Eng 18(3):215-32. https://doi.org/10.24191/jmeche.v18i3.15428

Donateo T, De Pascalis CL, Ficarella A (2018) Many-objective optimisation of mission and hybrid electric power system of unmanned aircraft. International Conference on the Application of Evolutionary Computation. p. 231-246. https://doi.org/10.1007/978-3-319-77538-8_17

CC BY

Gao X, Hou Z, Guo Z, Chen X (2015) Reviews of methods to extract and store energy for solar-powered aircraft. Renew Sustain Energy Rev 44:96-108. https://doi.org/10.1016/j.rser.2014.11.025

Hartney CJ (2011) Design of small solar-powered unmanned aerial vehicle [master's degree thesis]. San Jose: San Jose State University. https://doi.org/10.31979/etd.2nzx-arxy

Hosseini M, Nosratollahi M, Sadati H (2016) Evaluation of multidisciplinary design optimization methods and applying single level frameworks in unmanned aerial vehicle (UAV) design. Int J Sci Tech 9(47):1-7. https://doi.org/10.17485/ijst/2016/v9i47/101514

Ismail N, Norhashim N, Hamid SA, Kamal NLM, Sahwee Z, Shah SA, Yousoff WYW (2026) Solar energy materials and solar cells utilizing solar energy for UAVs: advancements, challenges and future perspectives in defense and military applications - A review. Sol Energy Mater Sol Cells 296:114075. https://doi.org/10.1016/j.solmat.2025.114075

Jia Q, Yu D (2025) Multi-objective task scheduling for earth observation insar satellites via non- dominated sorting student psychology based optimization algorithm. J Aerosp Technol Manag 17:e0325. https://doi.org/10.1590/jatm.v17.1362

Liu Y, Lv M, Sun K (2025) Comprehensive tradeoff and utilization of airborne renewable energy and uncertain stratospheric wind potential based on reinforcement learning. Energy 324:135932. https://doi.org/10.1016/j.energy.2025.135932

Mastoras P, Zkeri E, Panara A, Dasenaki ME, Maragou NC, Vakalis S, Fountoulakis MS, Thomaidis NS, Stasinakis AS (2023) Application of a pilot-scale solar still for wine lees management: characterization of by-products and valorization potential. J Environ Chem Eng 11(6):111227. https://doi.org/10.1016/J.JECE.2023.111227

Mattos BS, Secco NR, Salles EF (2013) Optimal design of a high-altitude solar- powered unmanned airplane. J Aerosp Technol Manag 5(3):349-61. https://doi.org/10.5028/jatm.v5i3.223

Montagnier O, Bovet L (2010) Optimisation of a solar-powered high altitude long endurance UAV. 27th International Conference of Aeronautic and Sciences. p. 1-10. https://hal.science/hal-01315480v1

Najafi Y (2001) Design of high altitude long endurance solar powered UAV [doctoral thesis]. San Jose State University. https://www.sjsu.edu/ae/docs/project-thesis/Najafi.S11.pdf?

Nguyen N Van, Maxim T, Park H, Kim S, Lee J (2013) A multidisciplinary robust optimization framework for UAV conceptual design. World Congress on Strutural and Multidisciplinary Optimisation. p. 19-25. https://doi.org/10.1017/S0001924000009027

Noth A, Engel W, Siegwart R (2006) Design of an ultra-lightweight autonomous solar airplane for continuous flight. In: Corke P, Sukkariah S (eds.) Field and service robotics. Berlin, Heidelberg: Springer. Springer Tracts in Advanced Robotics, v. 25. p. 441-52. https://doi.org/10.1007/11736592_37

Noth A, Siegwart R (2006) Design of solar powered airplanes for continuous flight. Zurich: Swiss Federal Institute of Technology. Retrieved from https://ethz.ch/content/dam/ethz/special-interest/mavt/robotics-n-intelligent-systems/asl-dam/documents/projects/Design_Skysailor.pdf

Papageorgiou A, Tarkian M, Amadori K, Ölvander J (2018) Multidisciplinary design optimization of aerial vehicles: a review of recent advancements. Int J Aerosp Eng 4258020. https://doi.org/10.1155/2018/4258020

Raymer DP (2007) Simplied aircraft design for homebuilders. Los Angeles: Design Dimension Press.

Reddy K, Sri B, Aneesh P, Bhanu K, Natarajan M (2016) Design analysis of solar-powered unmanned aerial vehicle. J Aerosp Technol Manag 8(4):397-407. https://doi.org/10.5028/jatm.v8i4.666

Safyanu BD, Abdullah MN, Omar Z (2019) Review of power device for solar-powered aircraft applications. J Aerosp Technol Manag 11:1-16. https://doi.org/10.5028/jatm.v11.1077

Safyanu BD, Omar Z, Abdullahi MN (2018) Review of photovoltaic cells for solar-powered aircraft applications. Int J Eng Technol 7(4):131-5. https://doi.org/10.14419/ijet.v7i4.25.22412.

Shiau J, Ma D, Chiu C, Shie J-R (2010) Optimal sizing and cruise speed determination for a solar-powered airplane. J Aircraft 47(2):622. https://doi.org/10.2514/1.45908

Sun K, Liu S, Gao Y, Du H, Cheng D, Wang Z (2025) Output power prediction of stratospheric airship solar array based on surrogate model under global wind field. Chin J Aeronaut 38(4):103244. https://doi.org/10.1016/j.cja.2024.09.020

Vieira S, Nascimento M, Barcelos D (2013) Multidisciplinary design optimization applied to the conceptual design of a small unmanned aerial vehicle. 10th World on Structural and Multidisciplinary Optimisation. p. 1-10. https://sigaa.unb.br/sigaa/public/docente/producao.jsf?siape=1652569

Wei X, Yao P, Xie Z (2020) Comprehensive optimization of energy storage and standoff tracking for solar-powered UAV. IEEE Syst J. 14(4):5133-43. https://doi.org/10.1109/JSYST.2020.2964579

Zhang L, Lv M, Meng J, Du H (2017) Optimization of solar-powered hybrid airship conceptual design. Aerosp Sci Technol 65:54-61. https://doi.org/10.1016/j.ast.2017.02.016

CC BY